RESEARCH ARTICLE | OCTOBER 21 2014

Vibronic structures in the visible luminescence of silica nanoparticles FREE

Luisa Spallino; Lavinia Vaccaro; Luisa Sciortino; Simonpietro Agnello; Marco Cannas; Franco Mario Gelardi; Roberto Boscaino

AIP Conf. Proc. 1624, 135–140 (2014)
https://doi.org/10.1063/1.4900469

Vibronic structures in the visible luminescence of silica nanoparticles

Luisa Spallino, Lavinia Vaccaro, Luisa Sciortino, Simonpietro Agnello, Marco Cannas, Franco Mario Gelardi and Roberto Boscaino

Dipartimento di Fisica e Chimica, Università degli Studi di Palermo, Via Archirafi 36 ,90123 PA, Italy

Abstract. Time resolved photoluminescence investigation in air and in vacuum atmosphere of the visible luminescence related to silica surface defects is here reported. Two contributions can be singled out: one, observed both in air and in vacuum, is the well-known blue band, peaked around 2.8 eV decaying in ∼5 ns; the other, only observed in vacuum, is a structured emission in the violet range characterized by two vibronic progressions spaced 1370 cm-1 and 360 cm^{-1} decaying in ∼100 ns. In contrast with previous attribution, the well distinguishable spectroscopic properties together with the observation of the effects induced by the interaction with nitrogen allow to state that the emission bands originate by two different defects.

Keywords: silica nanoparticles, surface defects, phonon-coupling, photoluminescence
PACS: 78.67.Bf; 73.20.Hb; 81.20.Fw; 78.47.Jd; 75.55.Qr; 78.30.Ly

INTRODUCTION

The modern optical applications require the use of high performance materials whose main properties must be, among other, small size and brightness [1, 2, 3]. The research is therefore aimed by the development of methods successful to easily produce highly luminescent nano-structured materials, controlling their chemical and physical characteristics [4, 5, 6]. Nano-structured silica is a system that well combines all these requirements: it is of facile synthesis and exhibits huge emissivity as a direct consequence of its dimensions. In fact, the nano-scale sizes entail a high specific surface area and then the presence of a wide variety of defects. Offering large accessibility to atomic and molecular species of the ambient atmosphere, the microscopic structure of these sites at the surface is also influenced by the environment [7].

Molecular oxygen, O_2, plays a crucial role since it is active in several reactions and it can diffuse through the nano-structured silica [8, 9]. Previous studies have demonstrated the formation of oxygen related defects by controlled thermochemical reactions. These peculiar surface defects, named dioxasilyrane, $Si(O_2)$, and silanone, Si=O, are characterized by a photoluminescence (PL) band in the visible range around 2.2-2.4 eV under UV excitation [7, 10]. In a recent work, O_2 oxygen molecule has also been proposed for a fast (few ns) emission centred around 2.8 eV (blue band) that, after vacuum treatment, is enriched by vibronic lines above 3.0 eV (violet) [11, 12]. The origin of the blue band has been associated with a faced defects pair consisting of $Si(O_2)$ and sylilene, Si••, its formation being induced by the dehydroxylation of adjacent geminal silanols (Si-OH) groups [13, 14]. On the basis of this model, it is suggested that the UV light causes the photolysis of the dioxasilyrane releasing O_2 in the excited state; the subsequent emission gives rise to the blue band coupled with the O_2 stretching phonon modes. To support this hypothesis, the close similarity with the PL observed in nano-crystals of Al_2O_3 (γ-alumina), an oxide structurally and compositionally different from amorphous silica nano-particles, was invoked. However the understanding of the excitation/emission pathway giving rise to this structured PL is currently debated [11, 12, 15, 16, 17].

This work deals with the emission properties of sol-gel synthesized nano-structured silica studied in air, nitrogen and vacuum environments. By means of the time-resolved photoluminescence technique, a detailed spectroscopic characterization was performed, leading to discern between the blue band and the vibronic emission. The effects induced by the interaction with nitrogen molecules confirm that the two emissions originate from two distinct luminescent defects.

Fundamentals and Applications in Silica and Advanced Dielectrics (SiO2014)
AIP Conf. Proc. 1624, 135-140 (2014); doi: 10.1063/1.4900469

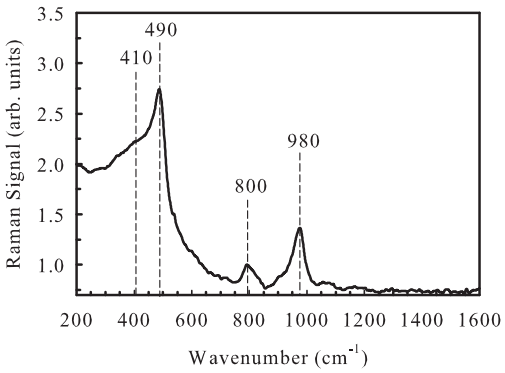

FIGURE 1. Raman spectrum of the synthesized material. Dashed lines indicate the position in cm^{-1} of the characteristic Raman active structures of nano-sized silica.

EXPERIMENTAL METHODS

Silica sample were synthesized using a modified St*ö*ber sol-gel route [18]. The colloidal solution was obtained mixing, 70 mmol of TEOS (Aldrich, 99.99%) with 0.3 mol of water, 0.4 mol of ethanol (Sigma-Aldrich, absolute $\geq$ 99.5%) and with 1.5 mmol of ammonium hydroxide (Sigma-Aldrich, 29% NH_3 basis). After stirring in ultrasonic bath for 40 minutes, the solution was centrifuged for one hour at 8000 rpm. The precipitate was separated by the supernatant and washed twice with water for one hour at 8000 rpm and one more time with acetone in the same conditions. The precipitate was finally dried for one week in ambient atmosphere. The resulting material is a white granular powder.

Structural information of the synthesized material was obtained by Fourier Transform (FT) -Raman spectroscopy. A Bruker RAMII FT-Raman Spectrometer, equipped with a 500 mW Nd:YAG laser (fundamental at 1064 nm), was employed.

The emission properties were investigated by the time-resolved PL technique. Tunable excitation pulsed light (pulse width $\sim$5 ns, repetition rate 10 Hz) was provided by a VIBRANT OPOTEK optical parametric oscillator laser system, pumped by the third harmonic (3.50 eV) of a Nd:YAG laser and equipped with a second harmonic generation crystal. The pulse energy was monitored with a pyroelectric detector and the Fluence/pulse was maintained at Φ=0.2 mJ/cm^2, low enough to avoid the generation of luminescent defects [19]. The emitted light was spectrally resolved by a monochromator (SpectraPro 2300i, PI/Acton) equipped with two gratings: one, with 150 grooves/mm and blazed at 300 nm, has a spectral resolution of 20 nm/mm; the other, with 300 grooves/mm and blazed at 500 nm, has a resolution of 10 nm/mm. The spectra were acquired by an intensified charge coupled device (CCD) camera driven by a delay generator (PI-MAX Princeton Instruments) that sets the delay time from the laser pulse, T_D, and the integration time of the emitted light, ΔT. The experimental set-up allows us to perform the experiments in controlled atmospheric conditions (air, nitrogen or vacuum) thanks to a cryostat connected to a vacuum pump that stabilizes the pressure down to 10^{-6}mbar. PL measurements were performed placing the sample in the cryostat in a standard front scattering geometry. All the emission spectra reported in this work are corrected for the monochromator dispersion.

RESULTS AND DISCUSSION

The FIGURE1 shows the Raman spectrum of the as synthesized material. As a fingerprint, it evidences the main typical features of nano-structured silica [20, 21]. The frequencies of the characteristic peaks are marked: ν=410 cm^{-1} is the bending mode of oxygen in n-membered rings (n>4) and it is usually known as R line; ν=490 cm^{-1} is the breathing mode of 4-membered rings, usually called D_1 line; ν=800 cm^{-1} is the SiO_2 network optical mode; ν=980 cm^{-1} is the vibration of (OH)-group with respect to Si. The absence in the Raman spectrum of the peak at ν=605 cm^{-1}, corresponding to the frequency of the 3-membered rings breathing mode (D_2 line), indicates that the synthesized material is porous [22, 23].

These structural features are consistent with a high specific surface material. Being able to accommodate a large

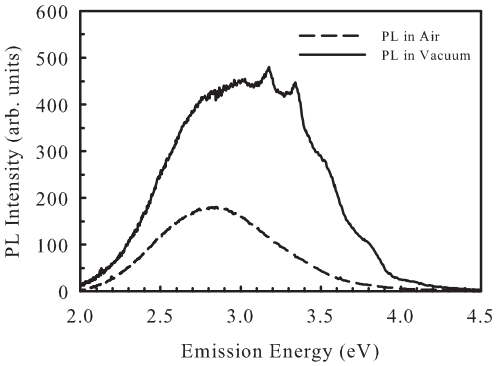

FIGURE 2. PL spectrum emitted by the sample stored in air (dashed line) and in vacuum for 24 hours (solid line). Both spectra are excited at E_{exc}=4.96 eV and acquired with T_D=16 ns and ΔT=100 ns.

number of surface defects, such a system is suitable to the purpose of this work. In fact, in ambient atmosphere one expects to observe, under UV excitation, the fast blue band related to surface defects in nano-sized silica systems [13]. In FIGURE2 the spectrum emitted by the sample in air is reported: it is excited at E_{exc}=4.96 eV and acquired setting T_D=16 ns and ΔT=100 ns. In agreement with previous studies [13, 14, 24, 25, 26], the silica sample emits a broad band centred at 2.80$\pm$0.02 eV, with a full width at half maximum (FWHM) of 0.80$\pm$0.03 eV. Being interested in the effect of the environment on this luminescence activity, we checked the PL after a storage in vacuum (P$\sim 10^{-5}$ mbar) for 24 hours. We note that the low pressure leads to the increase of the overall PL intensity and the appearance of a structured emission between 3.0 and 3.5 eV [12].

It is possible to single out two contributions thanks to the time-resolved PL technique combined with the tunable laser excitation. The results are summarized in FIGURE3 where the comparison between emission (a), excitation (b) and decay (c) properties related to the blue band in air and the structured emission in vacuum is reported. As concerns the emission characteristics, the opportune choice of the excitation energy and time acquisition parameters leads to the observation either of the blue band or the structured emission. This latter consists of a vibronic progression with four peaks spaced ΔE$\sim$0.17 eV ($\sim$1370 cm^{-1}), whose spectral positions are: 3.340$\pm$0.005 eV, 3.170$\pm$0.005 eV, 3.00$\pm$0.02 eV, 2.83$\pm$0.02 eV. Moreover, other PL peaks are observed at 3.290$\pm$0.005 eV and 3.245$\pm$0.005 eV. By the comparison of the excitation properties it is possible to clearly distinguish two different excitation profiles. The photoluminescence excitation (PLE) spectrum of the blue emission consists of two broad bands centered around E_{exc}=3.3$\pm$0.1 eV and E_{exc}=5.3$\pm$0.1 eV. The PLE pattern of the violet emission is also structured with two sharp peaks centered at 3.69$\pm$0.01 eV and 3.85$\pm$0.02 eV. The two emissions differ also in the decay kinetics: the blue band deviates from a pure exponential law; by a best fit analysis using a stretched exponential function $I(t) = I_0 exp[-(t/\tau)^{\gamma}]$, we get the lifetime τ=4.86$\pm$0.03 ns and stretching parameter γ=0.84$\pm$0.02. Also the structure PL follows a stretched exponential decay; we get the lifetime τ=90$\pm$2 ns and the stretching parameter γ=0.70$\pm$0.02.

In contrast with previous suggestions [11], the comparison between the emission, excitation and decay properties clearly proves that the structured PL and the blue band originate from two distinct defects. As concerns the structured PL, its excitation/emission pattern evidences a common vibronic progression with peaks spaced by ΔE$\sim$0.17 eV. This finding identifies a hard vibrational mode ($\nu_H \sim$1370 cm^{-1}) linearly coupled with the excitation and emission electronic transitions. The additional peaks in the PL spectrum spaced by 0.045 eV indicate that the electronic transition is also coupled with a soft vibrational mode of frequency $\nu_S \sim$360 cm^{-1}. To our knowledge this progression has not been resolved in previous works.

To further prove the different nature of the defects responsible for the blue emission and vibronic progression, we exposed the sample to nitrogen environment. In FIGURE4 the comparison between the two emission bands acquired in vacuum and nitrogen atmosphere is reported. The blue band is not affected by the presence of nitrogen whereas the structured PL undergoes a moderate quenching ($\sim$25%). It is worth to note that the peaks position remains the same and that the bleaching is reversible after restoring the vacuum (spectrum not reported). These findings indicate that the blue band and the structured emission have a distinguishable response to the N_2 environment thus confirming that they have a different source. Since this structured PL is peculiar to the vacuum, we can hypothesize that it originates from

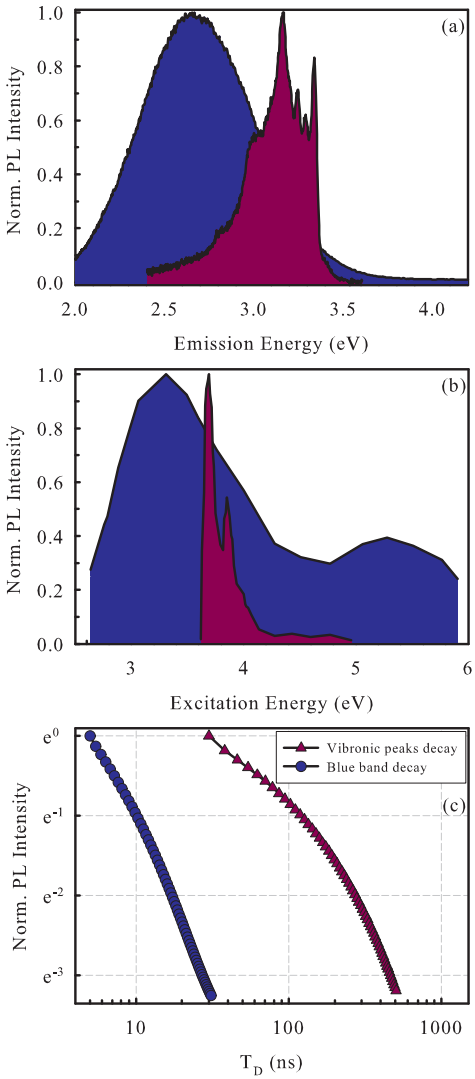

FIGURE 3. Comparison between the blue band (blue regions) and the vibronic structured (violet regions) emission properties monitored in air and in vacuum, respectively. (a) The acquisition parameters for blue PL are: E_{exc}=4.96 eV, T_D=10 ns, ΔT=100 ns. For the structured emission: E_{exc}=3.69 eV, T_D=115 ns and ΔT=250 ns. (b) The blue band PLE is obtained monitoring the maximum PL amplitude. The vibronic structured PLE is obtained monitoring the peak at 3.34 eV. (c) The blue band decay is monitored at E_{em}=2.8 eV. The acquisition parameters are: E_{exc}=4.96 eV, T_D from 5 ns to 31 ns , ΔT=1 ns. The structured PL decay is monitored at E_{em}=3.34 eV. The acquisition parameters are: E_{exc}=3.69 eV, T_D from 30 ns to T_D=505 ns, ΔT=25 ns.

a defect located at the surface: in air it weakly interacts with molecular species of the ambient atmosphere, such as nitrogen, so that the PL is quenched; the vacuum treatment removes these species, thus activating the optical emission.

CONCLUSIONS

The visible PL activity observed in a high specific surface silica based material under UV-Visible excitation is composed by two contributions: one, observed both in air and in vacuum, is the blue band, the other, peculiar

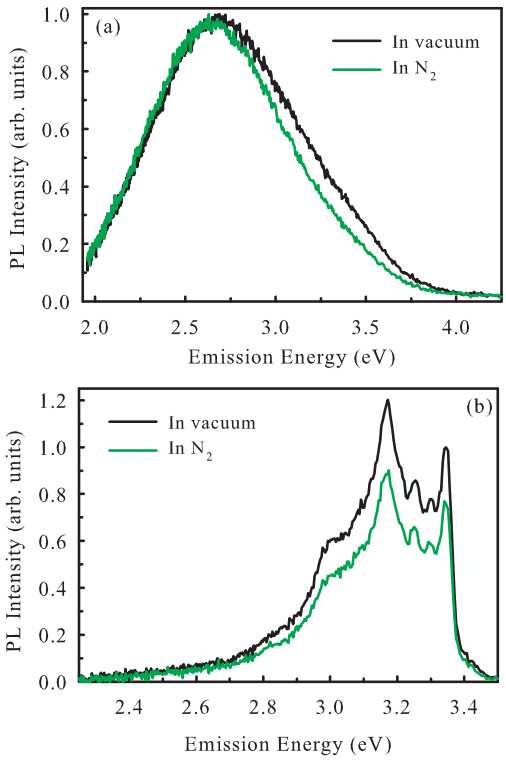

FIGURE 4. Effects induced by nitrogen purging on the PL. (a) Comparison between the blue band monitored in vacuum (black line) and under N_2 flux (green line). Both spectra are acquired exciting at E_{exc}=4.96 eV and setting T_D=10 ns and ΔT=10 ns. (b) Vibronic structures detected in vacuum (black line) and under N_2 atmosphere (green line). The spectra are excited at E_{exc}=3.69 eV and acquired with T_D=115 ns and ΔT=250 ns.

of vacuum, is a structured emission coupled with two vibration modes: a hard one ($\nu_H \sim 1370$ cm^{-1}) and a soft one ($\nu_S \sim 360$ cm^{-1}). On the basis of the emission, excitation and decay properties we assert that the structured luminescence and the blue band have a different origin. The effects induced on the two emissions by the different interaction with N_2 molecules prove this statement.

ACKNOWLEDGMENTS

The work was partially supported by FAE project, PO FESR Sicilia 2007/2013 4.1.1.1. and FFR 2012/2013 of University of Palermo. We express our gratitude to the group of the Laboratory of Advanced Materials Physics (Palermo University)(http://www. fisica.unipa.it//amorphous) for the stimulating discussions. G. Napoli and G. Tricomi are acknowledged for their technical assistance.

REFERENCES

1. S. Bonacchi, D. Genovese, R. Juris, M. Montalti, L. Prodi, E. Rampazzo, and N. Zaccheroni, *Angew. Chem. Int. Ed.* **50**, 4056 (2011).
2. C. Zhang, and J. Lin, *Chem. Soc. Rev.* **41**, 7938 (2012).
3. T. R. Alabi, D. Yuan, D. Bucknall, and S. Das, *Appl. Mater. Interfaces* **5**, 8932 (2013).
4. A. Rimola, D. Costa, M. Sodupe, J. Lambert, and P. Ugliengo, *Chem. Rev.* **113**, 4216 (2013).
5. J. M. McCrate, and J. G. Ekerdt, *Langmuir* **29**, 11868 (2013).

6. K. Kuroda, A. Shimojima, K. Kawahara, R. Wakabayashi, Y. Tamura, Y. Asakura, and M. Kitahara, *Chem. Mater.* **38**, 1255 (1988).
7. L. Vaccaro, A. Morana, V. Radzig, and M. Cannas, *J. Phys. Chem. C* **115**, 19476 (2011).
8. G. Renger, and B. Hanssum, *Photosynth. Res.* **102**, 487 (2009).
9. G. Iovino, S. Agnello, F. M. Gelardi, and R. Boscaino, *J. Phys. Chem. C* **116**, 11351 (2012).
10. V. N. Bagratashvili, S. I. Tsypina, V. A. Radtsig, A. O. Rybaltovskii, P. V. Chernov, S. S. Alimpiev, and Y. O. Simanovskii, *J. Non Cryst. Solids* **180**, 221 (1995).
11. A. Anjiki, and T. Uchino, *J. Phys. Chem. C* **116**, 15747 (2012).
12. L. Spallino, L. Vaccaro, L. Sciortino, S. Agnello, G. Buscarino, M. Cannas, and F. Gelardi, *Phys. Chem. Chem. Phys. DOI: 10.1039/C4CP02995J* (2014).
13. T. Uchino, N. Kurumoto, and N. Sagawa, *Phys. Rev. B* **73**, 233203 (2006).
14. A. Aboshi, N. Kurumoto, T. Yamada, and T. Uchino, *J. Phys. Chem. C* **111**, 8483 (2007).
15. A. Nishimura, S. Harada, and T. Uchino, *J. Phys. Chem. C* **114**, 8568 (2010).
16. C. M. Carbonaro, R. Corpino, P. C. Ricci, M. Salis, and A. Anedda, *J. Mater. Sci.* **48**, 4452 (2013).
17. C. M. Carbonaro, R. Corpino, P. Ricci, and D. Chiriu, *J. Non Cryst. Solids* **401**, 60 (2014).
18. T. St*ö*ber, and A. Fink, *J. Colloid Interface Sci.* **26**, 62 (1968).
19. L. Spallino, L. Vaccaro, S. Agnello, and M. Cannas, *J. Lumin.* **138**, 39 (2013).
20. T. Yamada, M. Nakajima, T. Suemoto, and T. Uchino, *J. Phys. Chem. C* **111**, 12973 (2007).
21. G. Vaccaro, S. Agnello, G. Buscarino, and F. M. Gelardi, *J. Phys. Chem. C* **114**, 13991 (2010).
22. C. J. Brinker, and G. W. Scherer, *SOL-GEL SCIENCE, The Physics and Chemistry of Sol-Gel Processing*, Academic Press, Inc., San Diego, 1990.
23. C. Kinowski, M. Bouazaoui, R. Bechara, L. L. Hench, J. M. Nedelec, and S. Turrell, *J. Non Cryst. Solids* **291**, 143 (2001).
24. L. Vaccaro, G. Vaccaro, S. Agnello, G. Buscarino, and M. Cannas, *Solid State Commun.* **150**, 2278 (2010).
25. C. Carbonaro, P. Ricci, R. Corpino, M. Marceddu, and A. Anedda, *J. Non Cryst. Solids* **357**, 1904 (2011).
26. G. L. Davies, J. McCarthy, A. Rakovich, and Y. K. Gun'ko, *J. Mater. Chem.* **22**, 7358 (2012).